Perceptual Learned Video Compression with Recurrent Conditional GAN

Ren Yang, Luc Van Gool, Radu Timofte

Computer Vision Laboratory, ETH Zurich, Switzerland {ren.yang, vangool, radu.timofte}@vision.ee.ethz.ch

Abstract

This paper proposes a Perceptual Learned Video Compression (PLVC) approach with recurrent conditional GAN. In our approach, we employ the recurrent auto-encoder-based compression network as the generator, and the most importantly, we propose a recurrent conditional discriminator, which judges raw and compressed video conditioned on both spatial and temporal features, including the latent representation, temporal motion and hidden states in recurrent cells. This way, in the adversarial training, it pushes the generated video to be not only spatially photo-realistic but also temporally consistent with groundtruth and coherent among video frames. The experimental results show that the proposed PLVC model learns to compress video towards good perceptual quality at low bit-rate, and outperforms the official HEVC test model (HM 16.20) and the previous learned approaches on several perceptual quality metrics and user studies. The codes will be released at the project page: https://github.com/RenYang-home/PLVC.

1 Introduction

The recent years have witnessed the increasing popularity of end-to-end learning-based image and video compression. Most existing models are optimized towards distortion, *i.e.*, PSNR and MS-SSIM. Recently, Generative Adversarial Network (GAN) has been used in image compression towards perceptual quality [Agustsson *et al.*, 2019; Mentzer *et al.*, 2020]. However, the study on efficient perceptual learned *video* compression still remains blank.

Different from image compression, generative video compression is a more challenging task. If borrowing the independent GAN of image compression to video, each frame is generated independently without temporal constraint, because the independent discriminator only pushes the spatial perceptual quality without considering temporal coherence. This may lead to the incoherent motion among video frames and thus the temporal flickering may severely degrade the perceptual quality.

To overcome these challenges, we propose a Perceptual Learned Video Compression (PLVC) approach with recur-

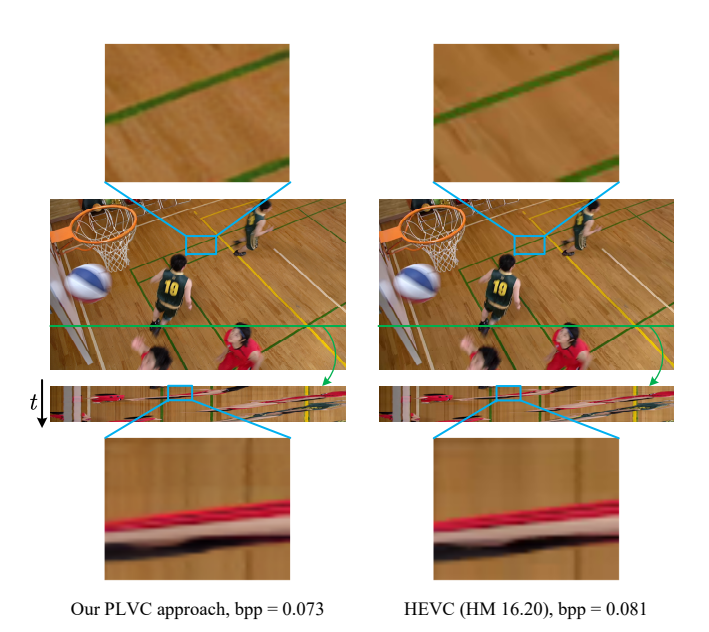


Figure 1: Example of the proposed PLVC approach in comparison with the official HEVC test model (HM 16.20).

rent conditional GAN, in which a recurrent generator and a recurrent conditional discriminator are trained in an adversarial way for perceptual compression. The recurrent generator contains recurrent auto-encoders to compress video and generate visually pleasing reconstructions in the adversarial training. More importantly, we propose a recurrent conditional discriminator, which judges raw and compression video conditioned on the spatial-temporal features, including latent representations, motion and the hidden states transferred through recurrent cells. Therefore, in the adversarial training, the discriminator is able to force the recurrent generator to reconstruct both photo-realistic and temporally coherent video, thus achieving good perceptual quality.

Figure 1 shows the visual result of the proposed PLVC approach on *BasketballDrill* (bpp = 0.0730) in comparison with the official HEVC test model HM 16.20 (bpp = 0.0813). The top of Figure 1 shows that our PLVC approach achieves richer and more photo-realistic textures than HEVC. At the bottom of Figure 1, we show the temporal profiles by vertically stacking a specific row (marked as green) along time steps. It can be seen that the result of our PLVC approach has comparable

temporal coherence with HEVC but has more detailed textures. As a result, we outperform HEVC on the perceptual quality at lower bit-rate. The contribution of this paper are summarized as:

- We propose a novel perceptual video compression approach with recurrent conditional GAN, which learns to compress video and generate photo-realistic and temporally coherent compressed frames.
- We propose the adversarial loss functions for perceptual video compression to balance the bit-rate, distortion and perceptual quality.
- The experiments (including user study) show the outstanding perceptual performance of our PLVC approach in comparison with the latest learned and traditional video compression approaches.
- The ablation studies show the effectiveness of the proposed adversarial loss and the spatial-temporal conditions in the proposed discriminator.

2 Related work

Learned image compression. In the past a few years, learned image compression has been attracting increasing interest. For instance, Ballé et al. proposed utilizing the variational auto-encoder for image compression and proposed the factorized [Ballé et al., 2017] and hyperprior [Ballé et al., 2018] entropy models. Later, the auto-regressive entropy models [Minnen et al., 2018; Lee et al., 2019; Cheng et al., 2019] were proposed to improve the compression efficiency. Recently, the coarse-to-fine model [Hu et al., 2020a] and the wavelet-like deep auto-encoder [Ma et al., 2020] were designed to further advance the ratedistortion performance. Besides, there are also the methods with RNN-based auto-encoder [Toderici et al., 2017; Johnston et al., 2018] or conditional auto-encoder [Choi et al., 2019] for variable rate compression. Moreover, Agustsson et al. [2019] and Menzter et al. [2020] proposed applying GAN for perceptual image compression to achieve photorealistic compressed images at low bit-rate.

Learned video compression. Inspired by the success of learned image compression, the first end-to-end learned video compression method DVC [Lu et al., 2019] was proposed in 2019. Later, M-LVC [Lin et al., 2020] extends the range of reference frames and beats the DVC baseline. Meanwhile, a plenty of learned video compression methods with bi-directional prediction [Djelouah et al., 2019], one-stage flow [Liu et al., 2020], hierarchical layers [Yang et al., 2020] and scale-space flow [Agustsson et al., 2020] were proposed. Besides, the content adaptive model [Lu et al., 2020], the resolution-adaptive flow coding [Hu et al., 2020b], the recurrent framework [Yang et al., 2021] and the feature-domain compression [Hu et al., 2021] were employed to further improve the compression efficiency. All these methods are optimized for PSNR or MS-SSIM. Veerabadran et al. [2020] proposed a GAN-based method for perceptual video compression, but has not outperformed x264 and x265 on LPIPS. Therefore, the video compression towards perceptual quality still has a large room to be studied.

3 Proposed PLVC approach

3.1 Motivation

GAN was first introduced by Goodfellow *et al.* [2014] for image generation. It learns to generate photo-realistic images by optimizing the adversarial loss

$$\min_{G} \max_{D} \mathbb{E}[f(D(\boldsymbol{x}))] + \mathbb{E}[g(D(G(\boldsymbol{y})))], \tag{1}$$

where f and g are scalar functions, and G maps the prior \mathbf{y} to $p_{\mathbf{x}}$. We define x as the groundtruth image and $\hat{\mathbf{x}} = G(\mathbf{y})$ as the generated image. The discriminator D learns to distinguish $\hat{\mathbf{x}}$ from \mathbf{x} . In the adversarial training, it pushes the distribution of generated samples $p_{\hat{\mathbf{x}}}$ to be similar to $p_{\mathbf{x}}$. As a result, G learns to generate photo-realistic images.

Later, the conditional GAN [Mirza and Osindero, 2014] was proposed to generate images *conditional* on prior information. Defining the conditions as *c*, the loss function can be expressed as

$$\min_{G} \max_{D} \mathbb{E}[f(D(\boldsymbol{x} \mid \boldsymbol{c}))] + \mathbb{E}[g(D(\hat{\boldsymbol{x}} \mid \boldsymbol{c}))]$$
(2)

with $\hat{x} = G(y)$. The goal of employing c in (2) is to push G to generate $\hat{x} \sim p_{\hat{x}|c}$ with the *conditional* distribution tending to be the same as $p_{x|c}$. In another word, it learns to fool D to believe that \hat{x} and x correspond to a shared prior c with the same conditional probability. By properly setting the condition prior c, the conditional GAN is expected to generate frames with desired properties, e.g., rich texture, temporal consistency and coherence, etc. This motivates us to propose a conditional GAN for perceptual video compression.

3.2 Framework

Figure 2 shows the framework of the proposed PLVC approach with recurrent conditional GAN. We define the raw and compressed frames as $\{x_i\}_{i=1}^T$ and $\{\hat{x}_i\}_{i=1}^T$, respectively. In our PLVC approach, we first estimate the motion between the current frame x_i and its previous compressed frame \hat{x}_{i-1} by the pyramid optical flow network [Ranjan and Black, 2017]. The motion is denoted as m_i , which is to be used in the recurrent generator (G) for compressing x_i and also to serve as one of the temporal conditions in the recurrent conditional discriminator (D). The architectures of G and D in our PLVC approach are introduced in the following.

Recurrent generator G. The recurrent generator G plays the role as a compression network. That is, given the reference frame \hat{x}_{i-1} and the motion m_i , the target frame x_i can be compressed by an auto-encoder-based DNN, which compresses x_i to latent representations y_i and outputs the compressed frame \hat{x}_i . In our PLVC approach, we employ the recurrent compression model RLVC [Yang $et\ al.$, 2021] as the backbone of G, which contains the recurrent auto-encoders to compress motion and residual, and the recurrent probability model P for the arithmetic coding of y_i . The detailed architecture of G is shown in the $Supplementary\ Material$.

Recurrent conditional discriminator D. The architecture of proposed recurrent conditional discriminator D is shown in Figure 2. First, we follow [Mentzer *et al.*, 2020] to feed y_i as the spatial condition to D. This way, D learns to distinguish the groundtruth and compressed frames based

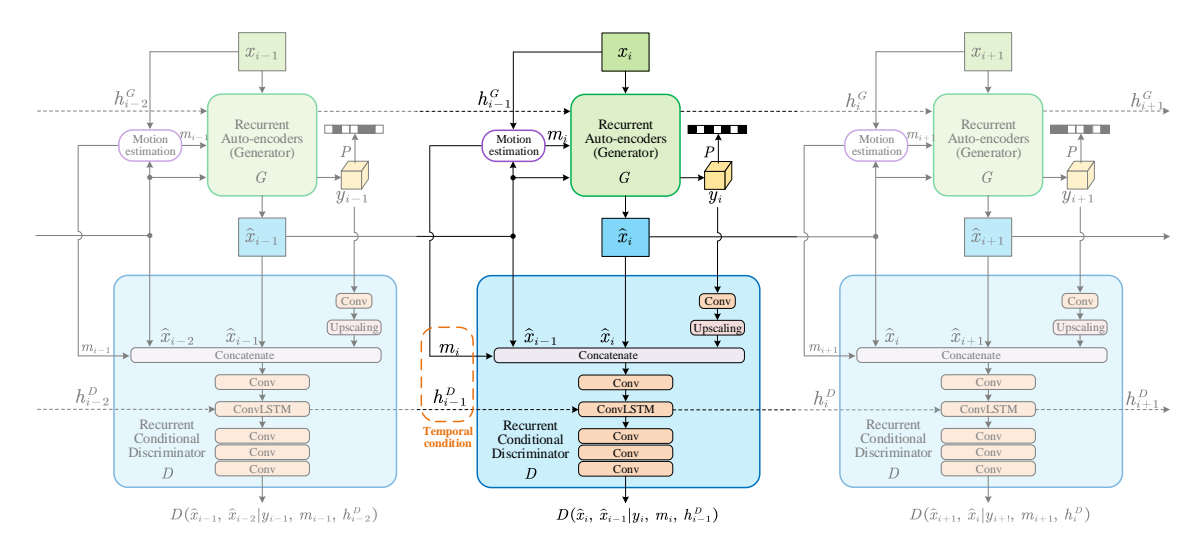


Figure 2: The proposed PLVC approach with recurrent GAN, which includes a recurrent generator G and a recurrent conditional discriminator D. The dash lines indicate the temporal information transferred through the recurrent cells in G and D.

on the shared spatial feature y_i , and therefore pushes G to generate \hat{x}_i with similar spatial feature to x_i .

More importantly, the temporal coherence is essential for visual quality. We insert a ConvLSTM layer in D to recurrently transfer the temporal information along time steps. The hidden state h_i^D can be seen as a long-term temporal condition fed to D, facilitating D to recurrently discriminate raw and compressed video taking temporal coherence into consideration. Furthermore, it is necessary to consider the temporal fidelity in video compression, i.e., we expect the motion between compressed frames is consistent with that between raw frames. For example, the ball moves along the same path in the videos before and after compression. Hence, we propose D to take as inputs the frame pairs (x_i, x_{i-1}) and $(\hat{x}_i, \hat{x}_{i-1})$ and make the judgement based on the same motion vectors m_i as the short-term temporal condition. If without the condition of m_i , G may learn to generate photo-realistic $(\hat{x}_i, \hat{x}_{i-1})$ but with incorrect motion between the frame pair. This leads to the poor temporal fidelity to the groundtruth video. It motivates us to include the temporal condition $m{m}_i$ as an input to the discriminator.

As such, we propose the discriminator D conditioned on spatial feature \boldsymbol{y}_i , short-term temporal feature \boldsymbol{m}_i and long-term temporal feature \boldsymbol{h}_{i-1}^D . Given these conditions, we have $\boldsymbol{c} = [\boldsymbol{y}_i, \boldsymbol{m}_i, \boldsymbol{h}_{i-1}^D]$ in (2) in our PLVC approach. The output of D can be formulated as $D(\boldsymbol{x}_i, \boldsymbol{x}_{i-1} \mid \boldsymbol{y}_i, \boldsymbol{m}_i, \boldsymbol{h}_{i-1}^D)$ and $D(\hat{\boldsymbol{x}}_i, \hat{\boldsymbol{x}}_{i-1} \mid \boldsymbol{y}_i, \boldsymbol{m}_i, \boldsymbol{h}_{i-1}^D)$ for raw and compressed samples, respectively. When optimizing the adversarial loss on sequential frames, the compressed video $\{\hat{\boldsymbol{x}}_i\}_{i=1}^T$ tends to have the same spatial-temporal feature as the raw video $\{\boldsymbol{x}_i\}_{i=1}^T$. Therefore, we achieve perceptual video compression with spatially photo-realistic and also temporally coherent frames. Please refer to the Supplementary Material for the detailed architecture of D.

It is worth pointing out that the effectiveness of the proposed D does not limit to a specific G, but has the generalizability to various compression networks. Please refer to the analyses and results in Section 4.5.

Table 1: The hyper-parameters for training PLVC models.

Quality	R_T (bpp)	λ	α_1	α_2	λ'	β
Low Medium High	$0.025 \\ 0.050 \\ 0.100$	$256 \\ 512 \\ 1024$	$3.0 \\ 1.0 \\ 0.3$	$0.010 \\ 0.010 \\ 0.001$	100 100 100	$0.1 \\ 0.1 \\ 0.1$

3.3 Training strategies

Our PLVC model is trained on the Vimeo-90k [Xue et al., 2019] dataset. Each clip has 7 frames, in which the first frame is compressed as an I-frame, using the latest generative image compression approach [Mentzer et al., 2020], and other frames are P-frames. To train the proposed network, we first warm up G on by the rate-distortion loss

$$\mathcal{L}_w = \sum_{i=1}^{N} R(\boldsymbol{y}_i) + \lambda \cdot d(\hat{\boldsymbol{x}}_i, \boldsymbol{x}_i).$$
(3)

In (3), $R(\cdot)$ denotes the bit-rate, and we use the Mean Square Error (MSE) as the distortion term d. Besides, λ is the hyperparameter to balance the rate and distortion terms.

Then, we propose training D and G alternately with the loss function combining the rate-distortion loss and the non-saturating [Lucic *et al.*, 2018] adversarial loss. Specifically, the loss functions are expressed as follows:

$$\mathcal{L}_{D} = \sum_{i=1}^{N} \left(-\log \left(1 - D(\hat{\boldsymbol{x}}_{i}, \hat{\boldsymbol{x}}_{i-1} | \boldsymbol{y}_{i}, \boldsymbol{m}_{i}, \boldsymbol{h}_{i-1}^{D}) \right) - \log D(\boldsymbol{x}_{i}, \boldsymbol{x}_{i-1} | \boldsymbol{y}_{i}, \boldsymbol{m}_{i}, \boldsymbol{h}_{i-1}^{D}) \right),$$

$$\mathcal{L}_{G} = \sum_{i=1}^{N} \left(\alpha \cdot R(\boldsymbol{y}_{i}) + \lambda' \cdot d(\hat{\boldsymbol{x}}, \boldsymbol{x}) - \beta \cdot \log D(\hat{\boldsymbol{x}}_{i}, \hat{\boldsymbol{x}}_{i-1} | \boldsymbol{y}_{i}, \boldsymbol{m}_{i}, \boldsymbol{h}_{i-1}^{D}) \right).$$
(4)

In (4), α , λ' and β are the hyper-parameters to control the trade-off of bit-rate, distortion and perceptual quality. We set three target bit-rates R_T to easily control the operating points,

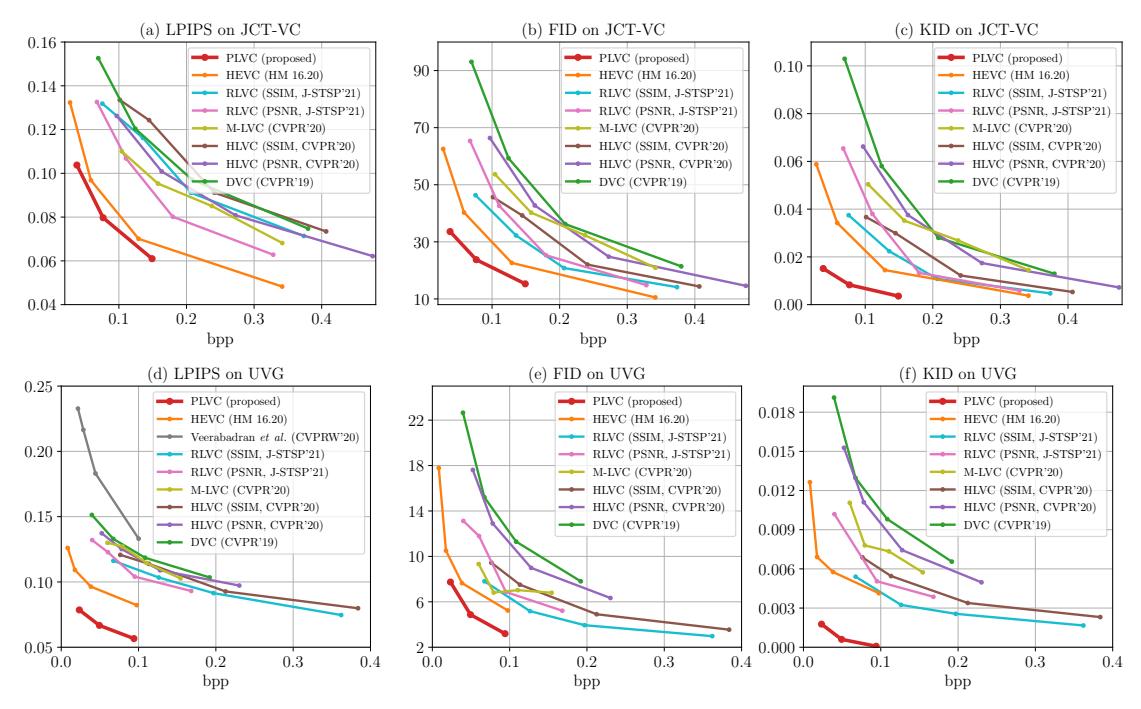


Figure 3: The numerical results on the UVG and JCT-VC datasets in terms of LPIPS, FID and KID.

and let $\alpha = \alpha_1$ when $R(y_i) \ge R_T$, and $\alpha = \alpha_2 \ll \alpha_1$ when $R(y_i) < R_T$. The hyper-parameters are shown in Table 1.

4 Experiments

4.1 Settings

We follow the existing methods to test on the JCT-VC [Bossen, 2013] (Classes B, C and D) and the UVG [Mercat et al., 2020] datasets. On perceptual metrics, we compare with the official HEVC model (HM 16.20)¹ and the latest open-sourced² learned video compression approaches DVC [Lu et al., 2019], HLVC [Yang et al., 2020], M-LVC [Lin et al., 2020] and RLVC [Yang et al., 2021], and the GAN-based method [Veerabadran et al., 2020]. We also report the MS-SSIM and PSNR results in comparison with plenty of existing approaches. Due to space limitation, some additional experiments are in the Supplementary Material.

4.2 Numerical performance

Perceptual quality. To numerically evaluate the perceptual quality, we calculate the Learned Perceptual Image Patch Similarity (LPIPS) [Zhang *et al.*, 2018], Fréchet Inception Distance (FID) [Heusel *et al.*, 2017] and Kernel Inception Distance (KID) [Bińkowski *et al.*, 2018] on our PLVC and compared approaches. In Figure 3, we observe that the proposed PLVC approach achieves good perceptual performance at low bit-rates, and outperforms all compared models in terms of all three perceptual metrics. Especially, our PLVC

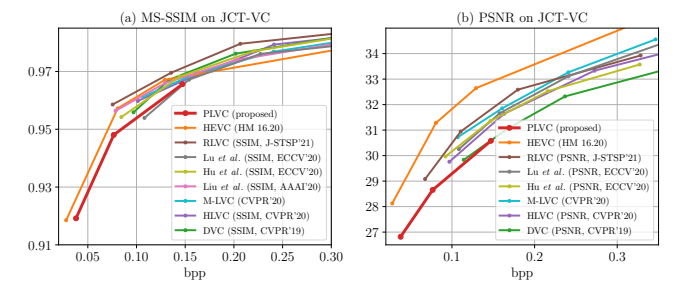


Figure 4: The MS-SSIM and PSNR results on JCT-VC.

approach reaches comparable or even better LPIPS, FID and KID values than other approaches which are at $2\times$ to $4\times$ bitrates of ours. It validates the effectiveness of the proposed method on compressing video towards perceptual quality.

Fidelity. Besides, Figure 4 shows that the MS-SSIM of our PLVC approach is better than DVC and comparable with Lu *et al.* [2020]. Our PSNR result also competes DVC. These verify that the proposed PLVC approach is able to maintain the fidelity to an acceptable degree when compressing video towards perceptual quality.

MS-SSIM vs. perceptual quality. MS-SSIM is more correlated with perceptual quality than PSNR, but it is still an objective metric. In Figure 4-(a), all learned methods (except M-LVC which does not provide the MS-SSIM-optimized model) are specifically trained by the MS-SSIM loss, resulting in higher MS-SSIM than the proposed PLVC. However, we have shown in Figure 3 that our PLVC approach has the best performance in terms of the perceptual metrics. Moreover, the user study in the following section also validates the outstanding perceptual performance of our PLVC approach. This also indicates that the perceptual metrics are better than MS-SSIM on evaluating perceptual quality.

¹We use the default Low-Delay P configuration of HM 16.20, since our approach does not have B-frame.

²Since the previous approaches do not report the results on perceptual metrics, we need to run the open-sourced codes to reproduce the compressed frames for perceptual evaluation.

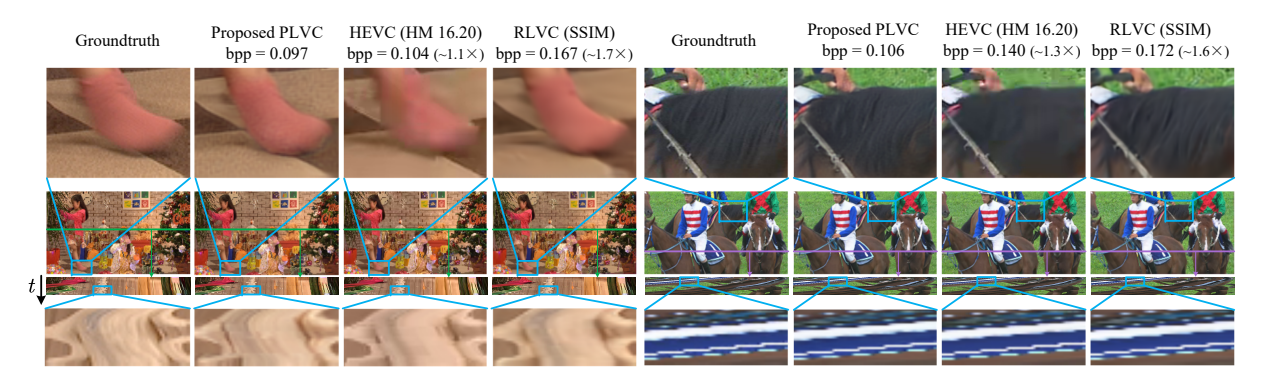


Figure 5: The visual results of the proposed PLVC approach, HM 16.20 and the MS-SSIM-optimized RLVC [Yang et al., 2021].

4.3 Visual results and user study

Figure 5 shows the visual results of our PLVC approach in comparison with HM 16.20 and the latest learned approach RLVC [Yang et al., 2021] (MS-SSIM optimized³). The top of Figure 5 illustrates the spatial textures, and the bottom shows the temporal profiles by vertically stacking the rows along time. It can be seen from Figure 5 that the proposed PLVC approach achieves richer and more photo-realistic textures at lower bit-rates than the compared methods. Besides, the temporal profiles indicate that our PLVC approach maintains the comparable temporal coherence with the groundtruth. More examples are Section 7.3 of the Supplementary Material.

We further conduct a MOS experiment with 12 non-expert subjects, who were asked to rate the compressed videos with the score from 0 to 100 according to subjective quality. Higher score indicates better perceptual quality. In this experiment, we compare with the official standard HM 16.20 and latest open-sourced⁴ method RLVC, which performs best in Figure 3. We use the MS-SSIM model of RLVC since MS-SSIM is more correlated with perceptual quality than PSNR.

The rate-MOS curves and the standard deviation of MOS on the JCT-VC dataset are shown in Figure 6. As we can see from Figure 6-(a), our PLVC approach successfully outperforms the official HEVC test model HM 16.20, especially at low bit-rates, and we are significantly better than the MS-SSIM-optimized RLVC. Besides, Figure 6-(b) shows that the standard deviation of MOS values of our PLVC approach is relatively lower than HM 16.20 and RLVC, indicating that the proposed PLVC model achieves more stable perceptual quality. In conclusion, these results verify that the subjects tend to consistently admire the better perceptual quality of our PLVC approach, in comparison with HM 16.20 and RLVC. We also provide the examples in video format in the *Project Page* for a more direct visual comparison.

4.4 Ablation studies

In ablation studies, we analyze the effectiveness of the generative adversarial network and the spatial-temporal conditions h_i^D , m_i and y_i . We provide the ablation analyses in Figure 9 in terms of both LPIPS and the MOS of an ablation user study with 10 non-expert subjects. Note that, the ablation user study in Figure 9 is conducted independently

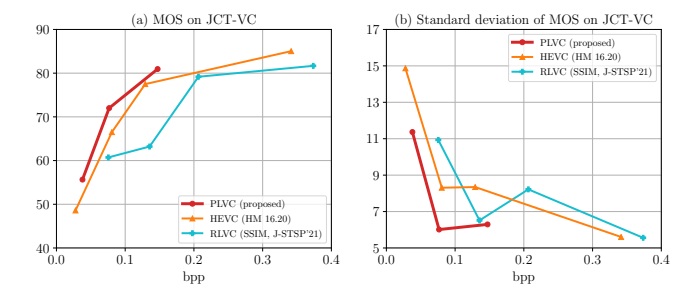


Figure 6: The rate-MOS result and its standard deviation.

after the user study in Figure 6, and the two user studies are conducted with different groups of subjects. Therefore, the MOS values in Figure 6 and Figure 9 can only be compared within each figure.

Generative adversarial network. We illustrate the results of the distortion-optimized PLVC model, denoted as PLVC (w/o GAN) in Figure 7, compared with the proposed PLVC approach. The model of PLVC (w/o GAN) is trained only until the convergence of (3) without the adversarial loss in (4). It can be seen from Figure 7 that the proposed PLVC approach achieves richer texture and more photo-realistic frames than PLVC (w/o GAN), even if when PLVC (w/o GAN) consumes $2\times$ to $3\times$ bit-rates. This is also verified by the LPIPS and MOS performance in Figure 9.

Temporal conditions in D. Then, we analyze the temporally conditional D. We first remove the recurrency in D, i.e., w/o h_i^D . As we can see from Figure 8, the temporal profile of PLVC (w/o h_i^D) (third column) is obviously distorted in comparison with the proposed PLVC approach and the groundtruth. As shown in Figure 9, the LPIPS and MOS performance of PLVC (w/o h_i^D) also degrades in comparison with the proposed PLVC model. Then, we further remove the temporal condition m_i from D and denote it as PLVC (w/o h_i^D , w/o m_i in D). As such, D becomes a normal discriminator which is independent along time steps. It can be seen from the right column of each example in Figure 8 that the temporal coherence becomes even worse when further removing the m_i condition in D. Similar result can also be observed from the quantitative and MOS results in Figure 9. These results indicate that the long-term and short-term temporal conditions h_i^D and m_i are effective to facilitate D to judge raw and compressed videos according to temporal coherence, in addition

³MS-SSIM is more correlated to perceptual quality than PSNR.

⁴We need the codes to reproduce the videos for the user study.

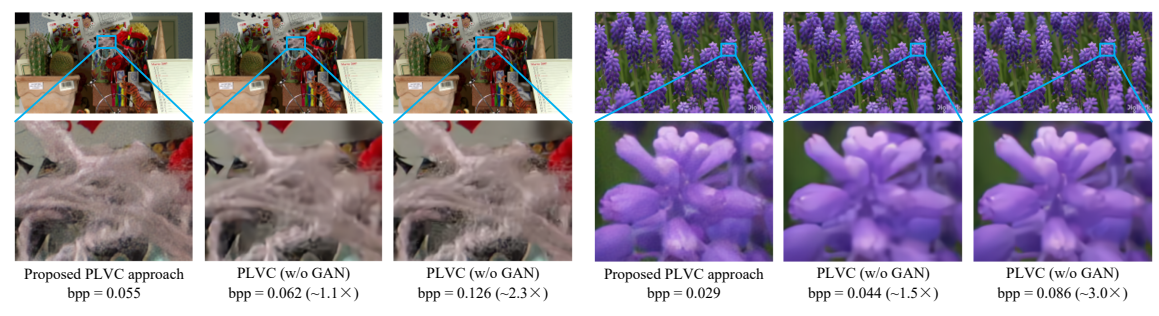


Figure 7: The ablation study on PLVC with and without GAN. (Zoom-in for better viewing)

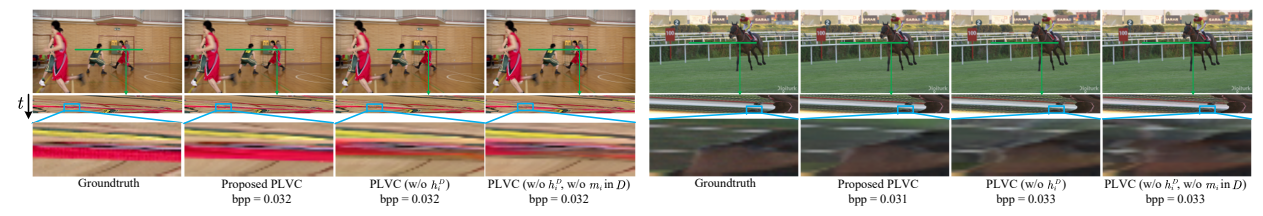


Figure 8: The temporal coherence of the ablation study on the temporal conditions h_i^D and m_i in D.

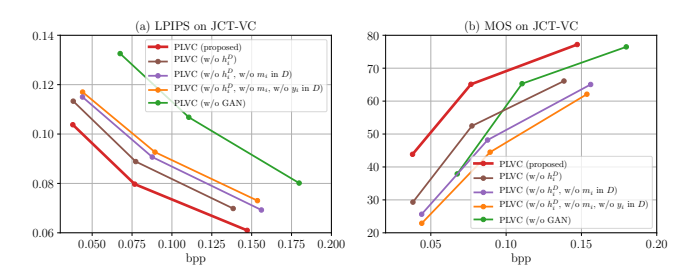


Figure 9: The LPIPS and MOS results of the ablation study. This MOS experiment is *independent from Figure 6 with different subjects*, so the MOS values can only be compared within each figure.

to the spatial texture. This way, it is able to force G to generate temporally coherent and visually pleasing video, thus resulting in good perceptual quality. We provide video examples of the ablation models in the $Project\ Page$ for a better visual comparison.

Note that, in Figure 9, the MOS values of PLVC (w/o \boldsymbol{h}_i^D) and PLVC (w/o \boldsymbol{h}_i^D , w/o \boldsymbol{m}_i in D) are even lower than PLVC (w/o GAN) at some bit-rates. This is probably because the incoherent frames generated by PLVC without temporal conditions \boldsymbol{h}_i^D and/or \boldsymbol{m}_i severely degrade the perceptual quality, making their perceptual quality even worse than the distortion-optimized model. It can be observed in the ablation video examples in the *Project Page*.

Spatial condition in D. Finally, we analyze the impact of the spatial condition y_i in D. Figure 9 shows that when further removing y_i from the conditions of D (denoted as PLVC (w/o h_i^D , w/o m_i , w/o y_i in D)), the performance in terms of LPIPS and MOS further degrades. This indicates the effectiveness of feeding y_i into D as the spatial condition. Please see Section 7.1 in *Supplementary Material* for the ablation visual results about the spatial condition.

4.5 Generalizability of the proposed D

Recall that in our PLVC approach, we utilize RLVC [Yang et al., 2021] as the backbone of G. However, the proposed

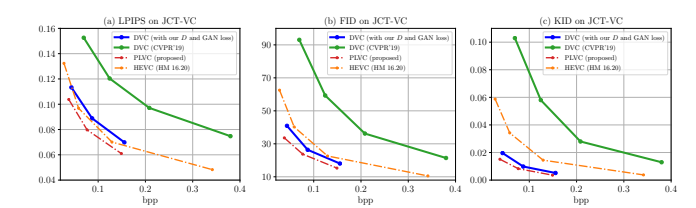


Figure 10: Applying the proposed D and GAN loss to DVC.

recurrent conditional discriminator D has the generalizability to various compression networks. For instance, Figure 10 shows the results of the DVC trained with the proposed D and GAN loss (blue curve) compared with the original DVC (green curve). It can be seen that the proposed D and GAN loss significantly improve the perceptual performance from the original DVC and make it outperform HM 16.20 on FID and KID. This verifies that the proposed perceptual video compression method does not limit to a specific compression network, but can be generalized to different backbones.

It is worth mentioning that the DVC trained with the proposed D performs worse than our PLVC model, because the DVC does not contain recurrent cells, while our PLVC model has a recurrent G which works with the recurrent conditional D, and they together make up the proposed recurrent GAN. This makes our PLVC approach outperforms the previous traditional and learned video compression approaches on LPIPS, FID, KID and MOS.

5 Conclusion

This paper proposes a recurrent GAN-based video compression approach. In our approach, the recurrent generator is trained with the adversarial loss to compress video with coherent and visually pleasing frames to fool the recurrent discriminator, which learns to judge the raw and compressed videos conditioned on spatial-temporal features. The numerical results and user studies validate the outstanding perceptual performance of the proposed method, compared with the standard HM 16.20 and learned video compression methods.

References

- [Agustsson *et al.*, 2019] Eirikur Agustsson, Michael Tschannen, Fabian Mentzer, Radu Timofte, and Luc Van Gool. Generative adversarial networks for extreme learned image compression. In *ICCV*, 2019.
- [Agustsson *et al.*, 2020] Eirikur Agustsson, David Minnen, Nick Johnston, et al. Scale-space flow for end-to-end optimized video compression. In *CVPR*, 2020.
- [Ballé *et al.*, 2017] Johannes Ballé, Valero Laparra, and Eero P Simoncelli. End-to-end optimized image compression. In *ICLR*, 2017.
- [Ballé *et al.*, 2018] Johannes Ballé, David Minnen, Saurabh Singh, Sung Jin Hwang, and Nick Johnston. Variational image compression with a scale hyperprior. In *ICLR*, 2018.
- [Bińkowski *et al.*, 2018] Mikołaj Bińkowski, Dougal J Sutherland, Michael Arbel, and Arthur Gretton. Demystifying MMD GANs. In *ICLR*, 2018.
- [Bossen, 2013] Frank Bossen. Common test conditions and software reference configurations. *JCTVC-L1100*, 2013.
- [Cheng *et al.*, 2019] Zhengxue Cheng, Heming Sun, Masaru Takeuchi, and Jiro Katto. Learning image and video compression through spatial-temporal energy compaction. In *CVPR*, 2019.
- [Choi *et al.*, 2019] Yoojin Choi, Mostafa El-Khamy, and Jungwon Lee. Variable rate deep image compression with a conditional autoencoder. In *ICCV*, 2019.
- [Djelouah *et al.*, 2019] Abdelaziz Djelouah, Joaquim Campos, Simone Schaub-Meyer, et al. Neural inter-frame compression for video coding. In *ICCV*, 2019.
- [Goodfellow *et al.*, 2014] Ian J Goodfellow, Jean Pouget-Abadie, Mehdi Mirza, et al. Generative adversarial nets. In *NeurIPS*, 2014.
- [Heusel *et al.*, 2017] Martin Heusel, Hubert Ramsauer, et al. GANs trained by a two time-scale update rule converge to a local nash equilibrium. In *NeurIPS*, 2017.
- [Hu *et al.*, 2020a] Yueyu Hu, Wenhan Yang, and Jiaying Liu. Coarse-to-fine hyper-prior modeling for learned image compression. In *AAAI*, 2020.
- [Hu *et al.*, 2020b] Zhihao Hu, Zhenghao Chen, Dong Xu, et al. Improving deep video compression by resolution-adaptive flow coding. In *ECCV*, 2020.
- [Hu *et al.*, 2021] Zhihao Hu, Guo Lu, and Dong Xu. Fvc: A new framework towards deep video compression in feature space. In *CVPR*, 2021.
- [Johnston *et al.*, 2018] Nick Johnston, Damien Vincent, David Minnen, et al. Improved lossy image compression with priming and spatially adaptive bit rates for recurrent networks. In *CVPR*, 2018.
- [Lee *et al.*, 2019] Jooyoung Lee, Seunghyun Cho, and Seung-Kwon Beack. Context-adaptive entropy model for end-to-end optimized image compression. In *ICLR*, 2019.
- [Lin *et al.*, 2020] Jianping Lin, Dong Liu, Houqiang Li, and Feng Wu. M-LVC: multiple frames prediction for learned video compression. In *CVPR*, 2020.

- [Liu *et al.*, 2020] Haojie Liu, Lichao Huang, Ming Lu, Tong Chen, and Zhan Ma. Learned video compression via joint spatial-temporal correlation exploration. In *AAAI*, 2020.
- [Lu *et al.*, 2019] Guo Lu, Wanli Ouyang, Dong Xu, et al. DVC: An end-to-end deep video compression framework. In *CVPR*, 2019.
- [Lu et al., 2020] Guo Lu, Chunlei Cai, Xiaoyun Zhang, et al. Content adaptive and error propagation aware deep video compression. In ECCV, 2020.
- [Lucic *et al.*, 2018] Mario Lucic, Karol Kurach, Marcin Michalski, et al. Are GANs created equal? A large-scale study. In *NeurIPS*, 2018.
- [Ma et al., 2020] Haichuan Ma, Dong Liu, Ning Yan, et al. End-to-end optimized versatile image compression with wavelet-like transform. *IEEE Transactions on Pattern Analysis and Machine Intelligence*, 2020.
- [Mentzer *et al.*, 2020] Fabian Mentzer, George D Toderici, Michael Tschannen, and Eirikur Agustsson. High-fidelity generative image compression. *NeurIPS*, 33, 2020.
- [Mercat *et al.*, 2020] Alexandre Mercat, Marko Viitanen, and Jarno Vanne. UVG dataset: 50/120fps 4K sequences for video codec analysis and development. In *ACM MM-Sys*, 2020.
- [Minnen *et al.*, 2018] David Minnen, Johannes Ballé, and George D Toderici. Joint autoregressive and hierarchical priors for learned image compression. In *NeurIPS*, 2018.
- [Mirza and Osindero, 2014] Mehdi Mirza and Simon Osindero. Conditional generative adversarial nets. *arXiv* preprint arXiv:1411.1784, 2014.
- [Ranjan and Black, 2017] Anurag Ranjan and Michael J Black. Optical flow estimation using a spatial pyramid network. In *CVPR*, 2017.
- [Toderici *et al.*, 2017] George Toderici, Damien Vincent, Nick Johnston, et al. Full resolution image compression with recurrent neural networks. In *CVPR*, 2017.
- [Veerabadran *et al.*, 2020] Vijay Veerabadran, Reza Pourreza, Amirhossein Habibian, and Taco S Cohen. Adversarial distortion for learned video compression. In *CVPR Workshops*, 2020.
- [Xue *et al.*, 2019] Tianfan Xue, Baian Chen, Jiajun Wu, Donglai Wei, and William T Freeman. Video enhancement with task-oriented flow. *International Journal of Computer Vision*, 127(8):1106–1125, 2019.
- [Yang et al., 2020] Ren Yang, Fabian Mentzer, Luc Van Gool, and Radu Timofte. Learning for video compression with hierarchical quality and recurrent enhancement. In *CVPR*, 2020.
- [Yang et al., 2021] Ren Yang, Fabian Mentzer, Luc Van Gool, and Radu Timofte. Learning for video compression with recurrent auto-encoder and recurrent probability model. *IEEE J-STSP*, 2021.
- [Zhang *et al.*, 2018] Richard Zhang, Phillip Isola, Alexei A Efros, et al. The unreasonable effectiveness of deep features as a perceptual metric. In *CVPR*, 2018.

Perceptual Learned Video Compression with Recurrent Conditional GAN - Supplementary Material -

Ren Yang, Luc Van Gool, Radu Timofte Computer Vision Laboratory, ETH Zurich, Switzerland

6 Detailed architectures

Figure 11 shows the detailed architecture of the recurrent generator G. In Figure 11, the convolutional layers are denoted as "Conv, filter size, filter number". GDN [Ballé $et\ al.$, 2017] and ReLU are the activation functions. Note that the layers with ReLU before Conv indicates the pre-activation convolutional layers. $\downarrow 2$ and $\uparrow 2$ are $\times 2$ downscaling and upscaling, respectively. In the quantization layer, we use the differentiable quantization method proposed in [Ballé $et\ al.$, 2017] when training the models, and use the rounding quantization for test. The Convolutional LSTM (ConvLSTM) layers in the autoencoders make the proposed G have the recurrent structure.

The detailed architecture of the proposed recurrent conditional discriminator D is illustrated in Figure 12. The denotations are the same as Figure 11. In D, we utilize the spectral normalization, which has been proved to be beneficial for discriminator. In the leaky ReLU, we set the leaky slope as 0.2 for negative inputs. Finally, the sigmoid layer is applied to output the probability in the range of [0,1].

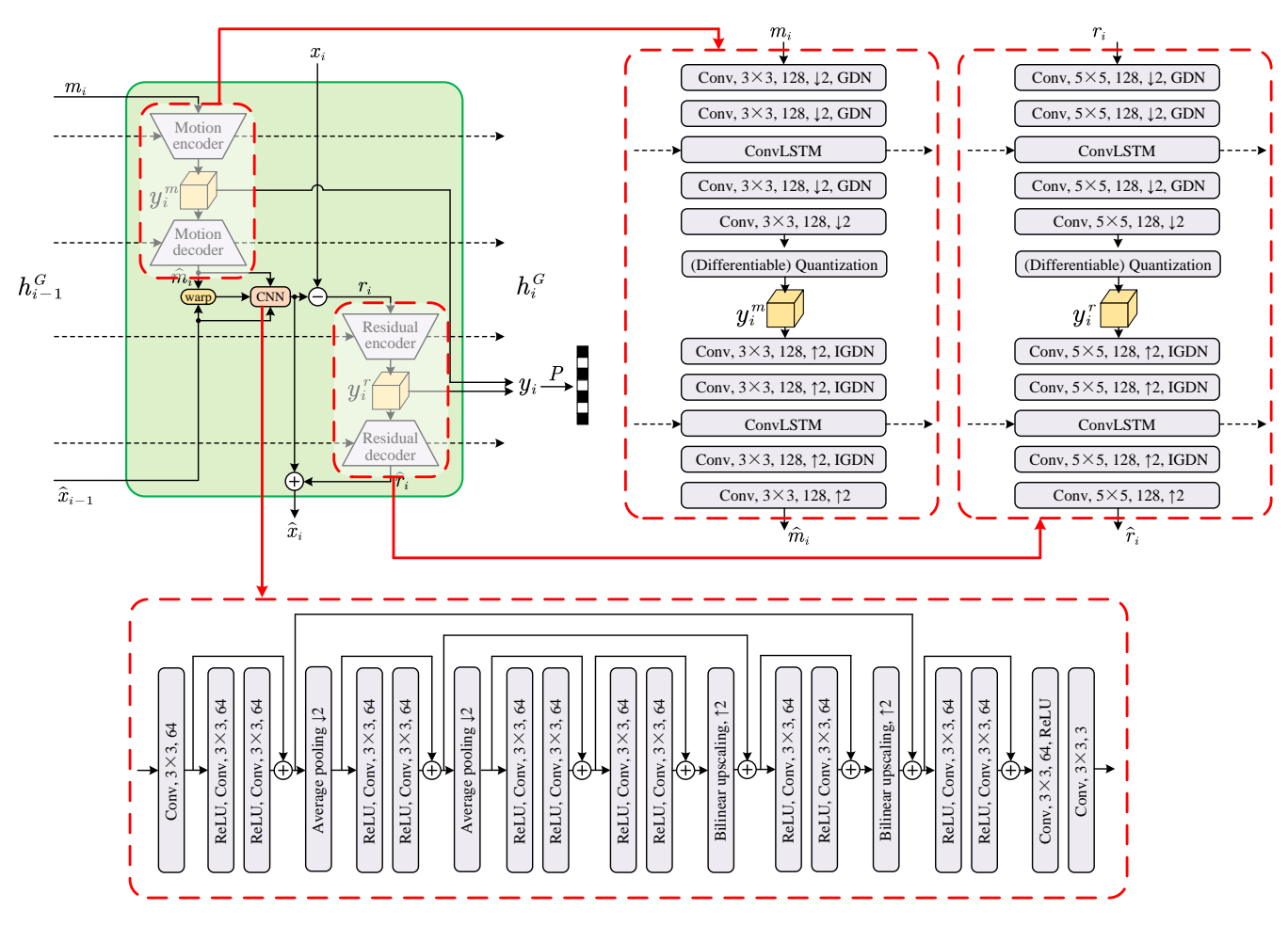


Figure 11: The detailed architecture of the recurrent generator G.

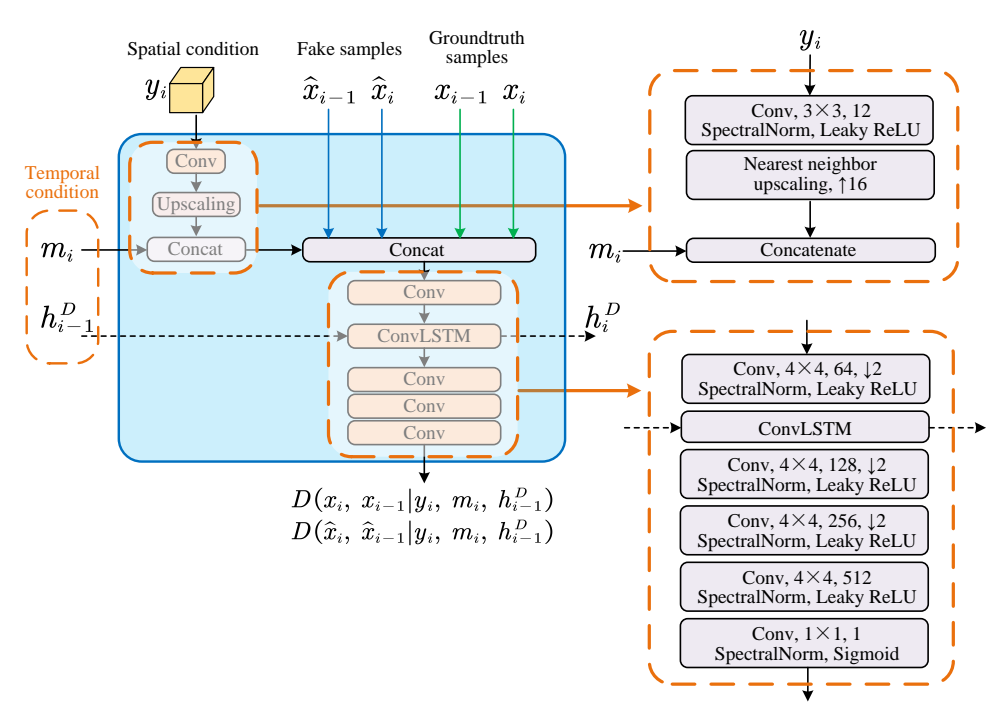


Figure 12: The detailed architecture of the recurrent conditional discriminator D.

7 More experimental results

7.1 Visual results for the ablation study of the spatial condition in D

Recall that in Section 4.4, we compared the LPIPS and MOS of PLVC (w/o h_i^D , w/o m_i in D) and the model that further removes y_i from the conditions of D, denoted as PLVC (w/o h_i^D , w/o m_i , w/o y_i in D). Due to the space limitation, we show the visual results in Figure 13 in this supplementary material. It can be seen from Figure 13, comparing with PLVC (w/o h_i^D , w/o m_i in D), the compressed frames generated by PLVC (w/o h_i^D , w/o m_i , w/o y_i in D) are with more artifacts and color shifting (see the right example in Figure 13), making them less similar to the groundtruth frames. This verifies that the spatial condition in D is effective for pushing the generator G to generate compressed frames with closer spatial feature with the groundtruth video, and therefore it ensures the fidelity of the compressed frames and also improves the visual quality.

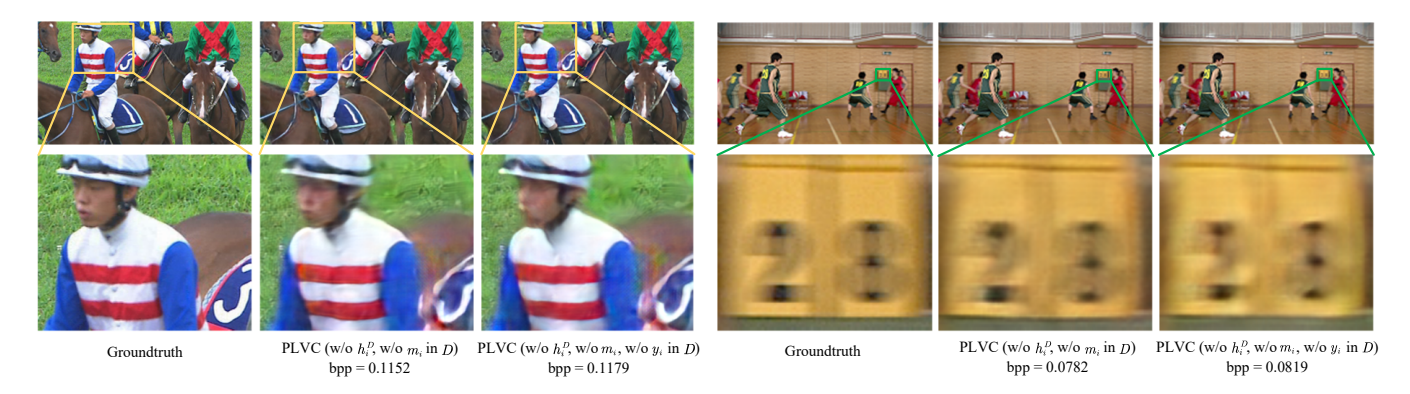


Figure 13: The visual results about the spatial condition in D.

7.2 Error propagation

In video compression, the IPPP frame structure may suffer from error propagation, but this has limited impact in the proposed method. First, the I-frame at the beginning of each GOP (9 frames including an I-frame and 8 P-frames) stops error propagation. Second, thanks to the recurrent structure of our method, the hidden states contain richer temporal prior when frame number increases. This is beneficial for compression performance, and hence it can combat error propagation. Figure 14 shows the average LPIPS-bpp curve of each P-frame in all GOPs in the JCT-VC dataset. It shows that there is no obvious performance degradation along time steps.

7.3 More visual results

We illustrate more visual results in Figure 15 (on the *last* page), which shows both spatial textures and temporal profiles of the proposed PLVC approach, HEVC (HM 16.20) and RLVC (MS-SSIM) [Yang *et al.*, 2021], in addition to Figure 5 in the main text. It can be seen from Figure 15, the proposed PLVC approach achieves more detailed and sharp textures than other methods, even if when HEVC consumes obviously more bit-rates and RLVC consumes more than $2\times$ bits. Besides, the temporal profiles also show that our PLVC approach has similar temporal coherence to the groundtruth, and the temporal profiles also show that we generate more photo-realistic textures than the compared methods. These results are consistent with the user study in Figure 6 of the main text, validating the outstanding perceptual performance of the proposed PLVC approach.

7.4 Time complexity

We conduct all training and test procedures on the TITAN Xp GPU with Debian GNU/Linux 10 system. The average encoding time on a 240p, 480p and 1080p frame is 0.063s (15.9 fps), 0.114s (8.8 fps) and 0.465s (2.2fps), respectively. The average decoding time on a 240p, 480p and 1080p frame is 0.031s (32.3 fps), 0.065s (15.4 fps) and 0.371s (2.7 fps), respectively. The training time of one model (including the warm up by MSE loss) takes around 170 hours.

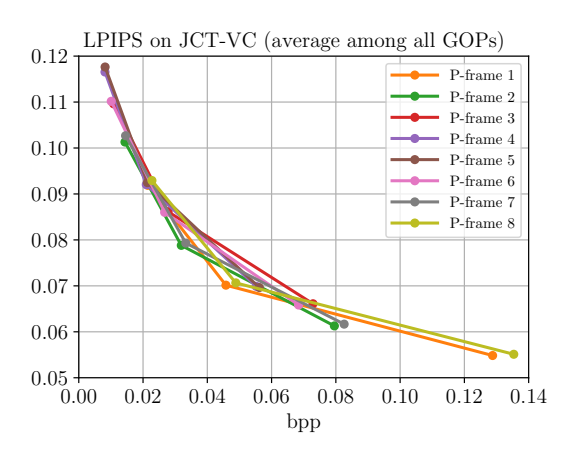


Figure 14: The average performance on LPIPS along time steps in the GOPs.

8 Video examples

We provide same examples of compressed videos for a direct visual comparison in the folder "Video_examples" in the *Project Page* at https://github.com/RenYang-home/PLVC. The files and the corresponding methods/models are listed in Table 2. The subfolder "Examples" include the video examples of the proposed PLVC approach, HM 16.20 and the MS-SSIM-optimized RLVC [Yang *et al.*, 2021]. The subfolder "Examples (ablation)" includes the results of the ablation models on the same video as "Examples", so the ablation results should be compared with the result of our PLVC approach in "Examples".

Table 2: The files and corresponding methods/models in video examples.

Examples				
1. Our PLVC bpp=xxx.mkv 2. RLVC (SSIM) bpp=xxx.mkv 3. HM16.20 bpp=xxx.bin	The proposed PLVC method The MS-SSIM-optimized RLVC method [Yang et al., 2021] The official HEVC test model HM 16.20			
Examples (ablation)				
4. PLVC (no h^D, no m_i) bpp=xxx.mkv 5. PLVC (no GAN) bpp=xxx.mkv	PLVC (w/o \boldsymbol{h}_i^D , w/o \boldsymbol{m}_i in D) PLVC (w/o GAN)			

Due to the size limitation, we show the first 100 frames of each method, and in the ablation video examples, we show the results of the two most important models PLVC (w/o h_i^D , w/o m_i in D) and PLVC (w/o GAN), which verify the effectiveness the proposed temporal condition in the discriminator and the effectiveness of the proposed GAN-based approach, respectively. Besides, since storing the compressed frames in PNG format significantly exceeds the size limitation, we first obtain the compressed frames of each model and then near-losslessly re-compress the frames by x265 as ".mkv" files to reduce the file size. For HM 16.20, we directly provide the bitstream (".bin" file) to save the space.

Note that, due to the near-losslessly re-compression by x265 for the ".mkv" files, the file sizes of the ".mkv" files do not indicate the bit-rate of the proposed and compared methods. The bit-rates are directly written in the file names. The ".mkv" files can be displayed by the VLC media player (https://www.videolan.org/index.zh.html). Note that since we store the compressed frames and then near-losslessly compress them by x265, the file sizes of the ".mkv" files do not indicate the bit-rate of the proposed and compared methods. The bit-rates are directly written in the file names. The ".bin" file of HM 16.20 can be viewed by the standard HEVC decoder, e.g., HM decoder.

9 Codes and reproducibility

To ensure the reproducibility, we will release all training and test codes with pre-trained models at https://github.com/RenYang-home/PLVC.

10 Broader impact and ethics statement

The generative video compression aims at compressing videos at low bit-rates and with good perceptual quality, which highly correlated with the Quality of Experience (QoE). Therefore, the study on perceptual video compression is meaningful for the efficient video transmission over the Internet with satisfied QoE.

Besides, since the traditional video coding standards, *e.g.*, HEVC, have been developed for several decades and are very well designed, the previous PSNR-optimized learned video compression methods are hard to compete with HM 16.20 in terms of PSNR. Thus, it is important to further explore the advantage of deep networks to seek a promising way to surpass the traditional codecs. The generative adversarial network and the adversarial training strategy are the strengths of deep learning, which can not be achieved by the handcrafted architectures. Therefore, the study on generative video compression plays to the strengths of deep networks, thus making it a promising direction to outperform the traditional video coding standards.

As far as we know, there is no ethical issues on the proposed method and the datasets in this paper.

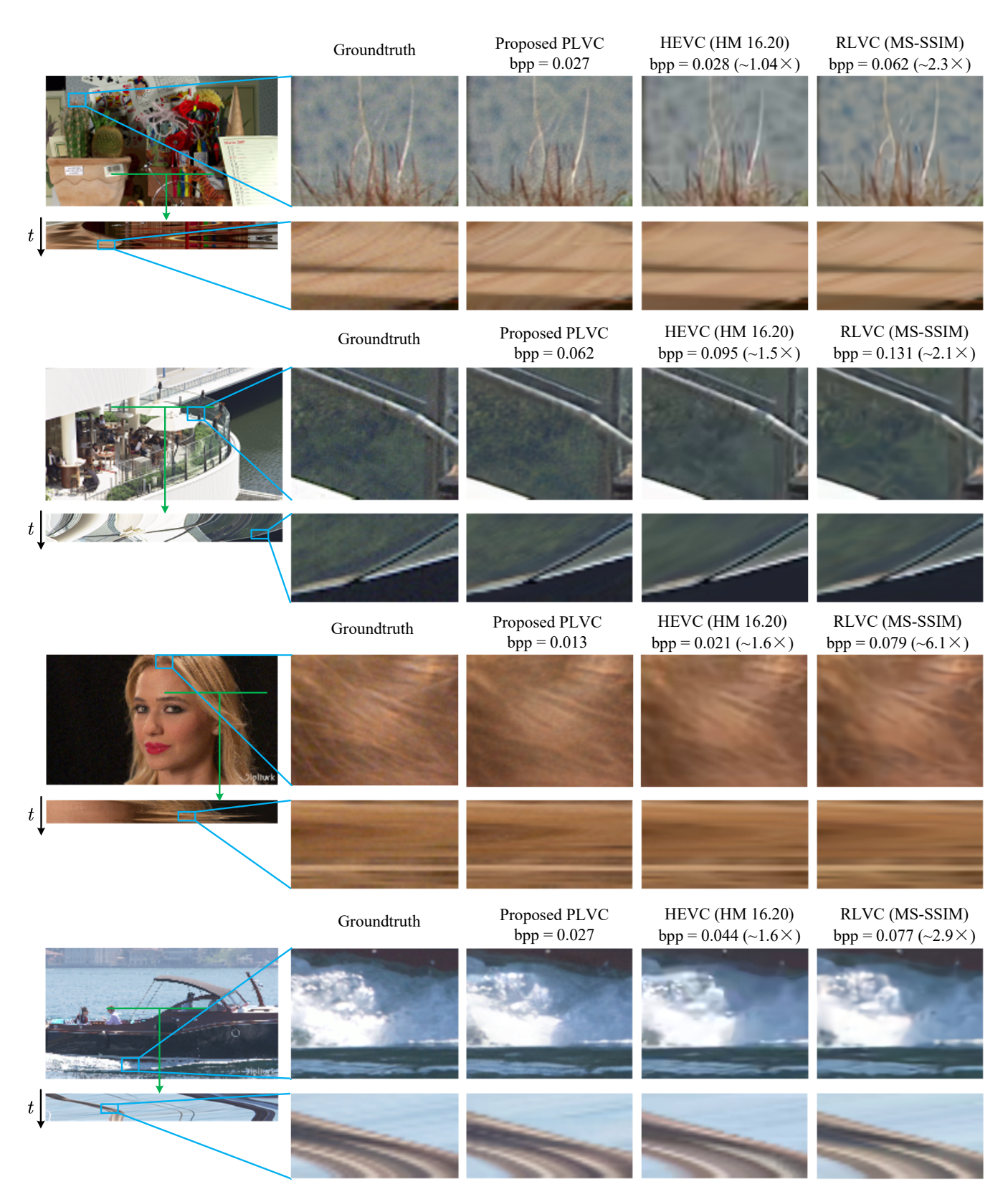


Figure 15: The visual results of the proposed PLVC approach in comparison with HM 16.20 and the MS-SSIM optimized RLVC [Yang et al., 2021]